Coordinated Operation of Parallel-Connected Inverters for Active Islanding Detection Using High Frequency Signal Injection

Fernando Briz, David Reigosa, Cristian Blanco, Juan Manuel Guerrero
University of Oviedo. Dept. of Elect., Computer & System Engineering, Gijón, 33204, Spain.
fernando@isa.uniovi.es, reigosa@isa.uniovi.es, blancocristian@uniovi.es, guerrero@isa.uniovi.es

Abstract: The high frequency impedance measured at the terminals of inverters connected in a microgrid by means of the injection of a small magnitude, high frequency voltage has been shown to be a reliable metric to detect islanding. While the implementation of this method is simple when only an inverter injects the high frequency signal, this case is of limited applicability. On the other hand, several concerns arise when multiple inverters work in parallel, primarily due to risk interference among inverters. Islanding detection using high frequency signal injection in microgrids with multiple parallel-connected inverters is studied in this paper. A strategy for the coordinated operation of the inverters without the need of communications or pre-established roles is proposed. Simulation and experimental results will be provided to demonstrate the viability of the concept.[1]

Index Terms— Islanding detection, grid impedance measurement, high frequency signal injection, distributed generation, smart grids.

I.- Introduction

Microgrids are becoming a key concept for the integration of Distributed generation (DG) based on renewable and non-renewable energy resources (photovoltaic, fuel cells, biomass, wind turbines, etc.), as well as Distributed storage (DS) systems. A feature of microgrids using DGs and DSs is that sources and loads can be distributed over a relatively large area. Because of the distributed nature, active elements of the microgrids should be controlled using local measurements, i.e. without dependence on communications systems [1].

Islanding detection is of special importance for the microgrid concept [2,3,14]. Islanding is defined as the situation in which DGs continue generating power when the microgrid is not connected to the utility grid. The requirements for islanding detection are regulated by local, regional and national authorities, standardizing institutions as IEEE and IEC also publishing recommendations for interconnecting distributed resources with the electric power systems [4-13]. Examples of these are the IEEE 1547 standard [4], the IEEE 929 standard [7], the UL 1741 standard [8] and the IEC standard [9], which require islanding detection in less than 2 seconds after the islanding condition occurs. The German standard DIN VDE 0126 [10] establishes that islanding detection methods should detect variations of the grid impedance of 1 Ohm in 2 seconds, 0.5 Ohm in 5 seconds being established by Austrian and Swiss standards [12,13].

Islanding detection methods can be classified into two groups: remote and local (inverter resident) [2,3,14].

Remote methods are based on communications between the grid and the DGs. They are highly flexible and with no risk of non-detection zone (NDZ). However, they are usually expensive due to the need of a communication infrastructure [14], also the risk of communication breakdown exists.

Local methods are based on data at the DGs site and are of two types: passive and active. Passive methods measure a system parameter (under/over voltage, under/over frequency, etc.) and compare it with a preset threshold. They are normally cheap to implement and grid friendly as no additional signal is injected. However, they present a large non-detection zone NDZ [14,15]. Active methods produce some kind of disturbance at the DGs output, and measure the grid response [14-24]. These methods have a lower NDZ but can negatively impact the power quality. Also interference among power converters trying to detect islanding simultaneously can occur.

Three potential scenarios can be considered for the evaluation of islanding detection methods [3]: 1) *Single inverter*; 2) *Multi-inverter* when multiple parallel connected inverters interact at one PCC and a major portion or all the power produced by the DGs is exported through the PCC; 3) *Microgrid* in which local loads can consume a significant amount or all the power produced by the DGs.

High frequency signal injection methods [17-22] are a type of local active methods. In these methods, a high frequency signal is injected via inverter, islanding being detected from the measured response. The implementation of these methods is easy in case 1) when only an inverter injects the high frequency voltage but is challenging in cases 2) and 3) as interference among inverters can occur. However, the fact that the injected signal has a frequency different from the grid frequency makes them suitable for case 3) even in the event that the DGs output power exactly matches the local loads and not power flows through the PCC.

This paper analyzes islanding detection using high frequency signal injection in grids with multiple parallel-connected inverters. To prevent interference, all the inverters participating in the strategy inject a synchronized high frequency signal. In order to minimize the impact of the high frequency signal on the grid, the inverters can behave either as *voltage sources* or as *current sources.* In addition, they have the ability to self-reconfigure their mode of operation depending on the microgrid/grid condition and without the need of communications or pre-established master/slave roles.

[1] This work was supported in part by the Research, Technological Development and Innovation Programs of the Ministry of Science and Innovation under grant MICINN-10-CSD2009-00046 and of the Spanish Ministry of Science and Innovation-ERDF under grant MICINN-10-ENE2010-14941.

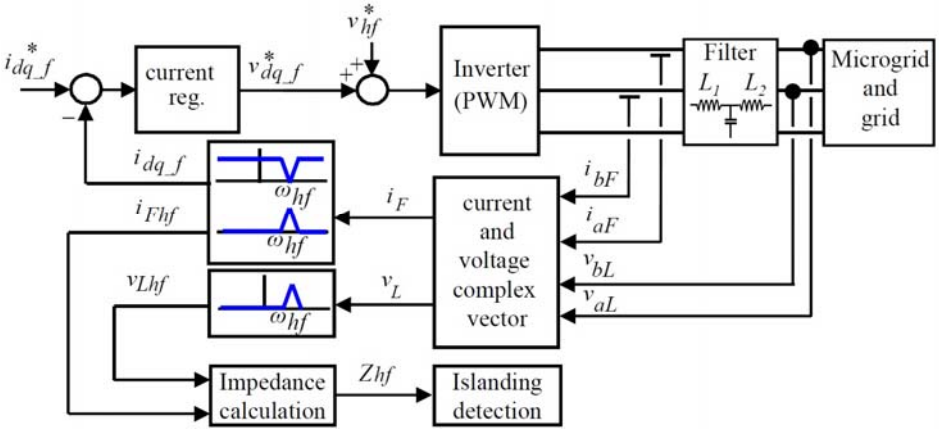

Fig. 1.- Block diagram of the master inverter.

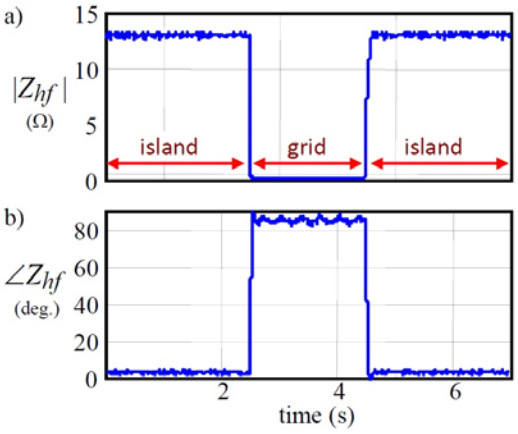

Fig. 2.- Experimentally measured high frequency impedance during island-grid transitions V_{hf}=1.5V, ω_{hf}=-333Hz.

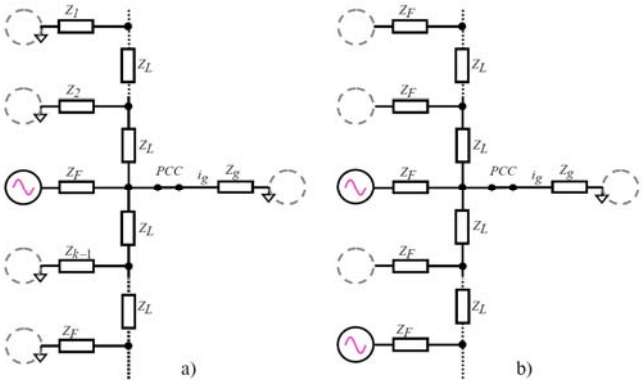

Fig. 3.- a) Static, single master inverter; b) Dynamic, multiple master inverter

II.- Islanding detection using high frequency voltage injection

Recently published works have shown that the high frequency impedance is a reliable metric to detect an islanding situation [17-22]. Voltage-source inverters (VSI) present in a microgrid (e.g. in controlled rectifiers used in APFs, back-to-back power converters, etc.) can easily inject a low-magnitude, high-frequency voltage from which the high frequency impedance is estimated. As an example, a rotating high frequency signal (1) can be injected, ω_{hf} and V_{hf} being the frequency and magnitude respectively. The induced high frequency current i_{Fhf} is given by (2). The high frequency impedance at the excitation frequency is Z_{hf} (3) with its phase angle being φ_Z.

$$v_{hf} = V_{hf}\, e^{\,j\theta hf} \quad ; \theta_{hf} = \int \omega_{hf}\, dt \tag{1}$$

$$i_{Fhf} = \frac{V_{hf}}{Z_{hf}}\, e^{\,j(\theta hf - \varphi z)} \tag{2}$$

$$Z_{hf} = R_{hf} + j\omega_{hf} L_{hf}\,; \; \varphi_z = \operatorname{atan}\left(\frac{\omega_{hf} L_{hf}}{R_{hf}}\right) \tag{3}$$

Fig. 1 shows the schematic implementation of the method. Fig. 2a and 2b show the magnitude and phase of the high frequency impedance Z_{hf} during a transition from island to grid and from grid to island. The change in both metrics between islanding and grid condition are readily observable. Islanding detection is based on the rate of variation of Z_{hf} with time, i.e. $\Delta Z_{hf}/\Delta t$. Comparison of Z_{hf} with a threshold might also potentially be used [21]. Further discussion on other forms of high frequency excitation as well as on the implementation of this method can be found in [21,22].

III.- Islanding detection using high frequency voltage injection for the case of multiple inverters

While simple for the case of a single inverter, the extension of the method described in Section II to the case of multiple inverters is not trivial. Strategies that have been proposed to address this case are presented in this section. In the discussion following *master inverters* refers to inverters

which inject a high frequency signal to detect the microgrid condition (grid/island). S*lave inverters* refers to inverters without such capability, but which still need to *know* the grid condition for their proper operation. This means that *master inverters* are responsible of *informing* the *slave inverters* on the grid condition. For the evaluation of the strategies, the following issues need to be taken into account:

- All the inverters in the microgrid participating in the strategy should *know* the microgrid condition (island/grid connected) within a time frame compatible with islanding detection standards.
- The adverse impact on the microgrid/grid power quality (THD) due to the injection of high frequency signals should be kept as small as possible and below the limits established by the connection standards [4-7].
- Use of separate communication channels is not allowed.
- The injection of an additional high frequency signal for communication purposes is acceptable as this does not have the problems/concerns intrinsic to communications, like cost and the risk of communication breakdown. Details on the use of the secondary high frequency signal can be found in [21,22].

a) Static, single master inverter

In [21], the use of a master inverter, responsible of injecting a high frequency rotating voltage vector (1) was proposed. The rest of inverters in the microgrid were configured to be slaves. Two high frequency signals were injected by the master inverter: the first one for islanding detection as described in Section II; the second one to communicate the islanding condition to the rest of (slave) inverters present in the microgrid. Fig. 3a schematically shows the high frequency model for this case. The inverter closer to the PCC injects the high frequency voltage, therefore behaving like a voltage source. Contrary to this, the rest of inverters as well as the grid voltage do not contain a high frequency voltage component, being modeled therefore as an impedance connected to ground.

The implementation of this strategy is simple as no interference among inverters can occur –only the master inverter injects high frequency signals–. However, it has several limitations:

- Failure of the master inverter would leave the grid without the high frequency signal voltage, the rest of inverters in the grid hence losing their capability to detect islanding.
- The location of the master inverter has to be carefully chosen in large microgids. For inverters located far from the PCC, the variation of the high frequency impedance between grid and island condition might be small, reducing the reliability of the method.
- Inverters including high bandwidth current regulators, e.g. active filters, might *see* the high frequency signal as a disturbance and partially compensate for it.

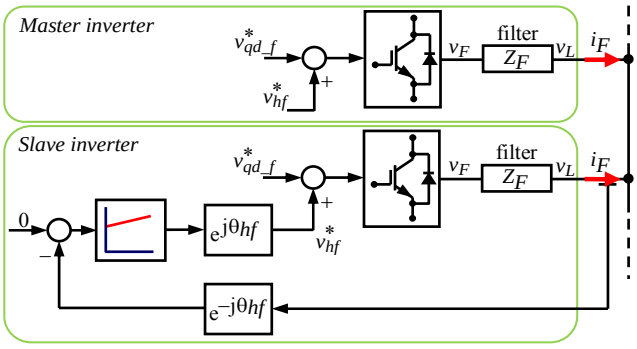

Fig. 4.- Schematic representation of the *master* and *slave* inverters implementing the infinite impedance mode. Current regulators needed for the control of the fundamental current are not shown (see Fig. 1 for details)

b) Dynamic (multiple) master inverter

In [22], a dynamic master assignment strategy was proposed. The signal injection by the master inverter is as in the previous case and islanding is detected from the high frequency impedance, as described in Section II. Slave inverters include a high frequency PI current regulator to prevent their reaction against the high frequency current (see Fig. 4). By making its command equal to zero, it is guaranteed that no high frequency current circulates through the slave inverters output. This mode of operation was named *infinite impedance*. Slave inverters detect islanding/grid connected condition from the changes in their high frequency current regulator output voltage $v^*_{hf\_s}$. This also enables slave inverters detect failure of the master inverter; i.e. if $v^*_{hf\_s} = 0$ means that there is no master inverter injecting the high frequency voltage. This master-slave strategy has several appealing properties.

- The high frequency voltage injected by the master inverter is not corrupted by the reaction of other inverters.
- Slave inverters automatically detect failure of the master inverter. A competitive strategy for the reassignment of the master inverter role in the event of master inverter failure was defined in [22].
- The master-inverter reassignment strategy naturally allows multiple master inverters. Slave inverters being too far from the master inverter might be unable to detect master's high frequency signal voltage. This will automatically trigger a competitive process to become master. As a result, several master inverters distributed all over the microgrid can operate simultaneously.

Fig. 3b schematically shows the high frequency model for this case. Master inverters behave like voltage sources. Slave inverters, due to their *infinite impedance* configuration, behave as an open circuit. As for the case in Fig. 3a, the grid is modeled as a ground connected impedance.

Regardless of its appealing characteristics this strategy also has some limitations:

- The modes of operation of operation of master and slave inverters differ substantially (see Fig. 4, [21,22]).

Switching between both modes is triggered by the presence/absence of the high frequency voltage in the microgrid. Though the filtering to detect the presence of the high frequency voltage is relatively simple [21], its implementation can be problematic in practice. The signals can be corrupted by noise in the acquisition system, harmonics in the voltages due to non-linear loads, transients, etc. Spurious detection of the high frequency voltage might result in repeated master/slave transitions, with unpredictable results.

- For a given magnitude of the injected high frequency voltage at the filter output, the resulting high frequency component of the filter current i_{Fhf} (4) will be function of the high frequency voltage v_{Fhf}, the output filter impedance Z_F and the equivalent high frequency impedance at the point of connection of the inverter to the microgrid Z_{hf}.

$$i_{Fhf} = \frac{v_{Fhf}}{Z_F + Z_{hf}} \tag{4}$$

While v_{Fhf} and Z_F are known in advance, significant uncertainty exists regarding Z_{hf}. For inverters close to the PCC in grid operation, this impedance can be very small and the circulating high frequency current i_{Fhf} large, adversely impacting the power quality (THD).

To overcome aforementioned limitations, a strategy for the coordinated operation of multiple parallel connected inverters in a microgrid is proposed in the following section.

$$\begin{bmatrix} v_{hf1} \\ 0 \\ 0 \\ 0 \\ v_{hf2} \\ 0 \\ 0 \\ 0 \\ \cdots \\ v_{hfN-1} \\ 0 \\ 0 \\ 0 \\ v_{hfN} \\ 0 \\ 0 \\ 0 \end{bmatrix} = \begin{bmatrix} Z_{F1} & 1 & 0 & 0 & 0 & 0 & 0 & 0 & 0 & 0 & \cdots & 0 & 0 & 0 & 0 & 0 & 0 \\ 1 & 0 & -1 & -1 & 0 & 0 & 0 & 0 & 0 & 0 & \cdots & 0 & 0 & 0 & 0 & 1 & 0 \\ 0 & 1 & -Z_{L12} & 0 & 0 & -1 & 0 & 0 & 0 & 0 & \cdots & 0 & 0 & 0 & 0 & 0 & 0 \\ 0 & 1 & 0 & -Z_{l1} & 0 & 0 & 0 & 0 & 0 & 0 & \cdots & 0 & 0 & 0 & 0 & 0 & 0 \\ 0 & 0 & 0 & 0 & Z_{F2} & 1 & -1 & 0 & 0 & 0 & \cdots & 0 & 0 & 0 & 0 & 0 & 0 \\ 0 & 0 & 1 & 0 & 1 & 0 & -1 & -1 & 0 & 0 & \cdots & 0 & 0 & 0 & 0 & 0 & 0 \\ 0 & 0 & 0 & 0 & 0 & 1 & -Z_{L23} & 0 & 0 & -1 & \cdots & 0 & 0 & 0 & 0 & 0 & 0 \\ 0 & 0 & 0 & 0 & 0 & 1 & 0 & -Z_{l2} & 0 & 0 & \cdots & 0 & 0 & 0 & 0 & 0 & 0 \\ \cdots & \cdots & \cdots & \cdots & \cdots & \cdots & \cdots & \cdots & \cdots & \cdots & \cdots & \cdots & \cdots & \cdots & \cdots & \cdots & \cdots \\ 0 & 0 & 0 & 0 & 0 & 0 & 0 & 0 & 0 & 0 & \cdots & 0 & 0 & 0 & 0 & 0 & 0 \\ 0 & 0 & 0 & 0 & 0 & 0 & 0 & 0 & 0 & 0 & \cdots & -1 & -1 & 0 & 0 & 0 & 0 \\ 0 & 0 & 0 & 0 & 0 & 0 & 0 & 0 & 0 & 0 & \cdots & -Z_{LN-1N} & 0 & 0 & -1 & 0 & 0 \\ 0 & 0 & 0 & 0 & 0 & 0 & 0 & 0 & 0 & 0 & \cdots & 0 & -Z_{LN} & 0 & 0 & 0 & 0 \\ 0 & 0 & 0 & 0 & 0 & 0 & 0 & 0 & 0 & 0 & \cdots & 0 & 0 & Z_{FN} & 1 & 0 & 0 \\ 0 & 0 & 0 & 0 & 0 & 0 & 0 & 0 & 1 & 0 & \cdots & 1 & 0 & 1 & 0 & -1 & -1 \\ 0 & -1 & 0 & 0 & 0 & 0 & 0 & 0 & 0 & 0 & \cdots & 0 & 0 & 0 & 1 & -Z_{LN1} & 0 \\ 0 & 0 & 0 & 0 & 0 & 0 & 0 & 0 & 0 & 0 & \cdots & 0 & 0 & 0 & 1 & 0 & -Z_{lN} \end{bmatrix} \begin{bmatrix} i_{Fhf1} \\ v_{Lhf1} \\ i_{Lhf12} \\ i_{lhf2} \\ i_{Fhf2} \\ v_{Lhf2} \\ i_{Lhf23} \\ i_{lhf3} \\ \cdots \\ i_{FhfN-1} \\ v_{LhfN-1} \\ i_{LhfN-1N} \\ i_{lhfN-1} \\ i_{lhfN} \\ v_{LhfN} \\ i_{LhfN1} \\ i_{lhfN} \end{bmatrix} \tag{5}$$

IV.- Islanding detection in microgrids with multiple inverters using combined current/voltage injection

Most of signal injection based islanding detection methods that have been proposed inject a high frequency voltage. The island/grid condition is estimated from the resulting high frequency impedance. However, it is also possible to inject a high frequency current. Deciding between voltage and current injection can be based on the high frequency impedance seen by the inverter. Voltage injection would be advantageous during island operation or for inverters located far from the PCC. In these cases, the equivalent impedance seen by the inverter will be large, limiting the resulting high frequency current. On the contrary, for inverters operating near the PCC during grid operation, the equivalent impedance will be small. Current injection would be advantageous in this case, since voltage injection would result in a relatively large high frequency current. Combining high frequency voltage injection and high frequency current injection would therefore be advisable for inverters experiencing large variations in the high frequency impedance seen at their terminals, as would be the case of inverters located near the PCC.

Islanding detection using combined voltage/current injection is analyzed in this section. In the proposed strategy all the inverters synchronously inject a high frequency signal. The inverters dynamically readapt their mode of operation between voltage and current injection, according to their location and to the grid condition. The model used for the analysis is first presented. Combined voltage/current injection, synchronization of the high frequency signals and parallel operation of inverters are analyzed in further subsections.

a) Grid model

The microgrid model shown in Fig. 5 will be used for analysis and simulation purposes. It is observed that the microgrid has a ring configuration, with node *k* being the point of common coupling (PCC). The mathematical model of the

grid is given by (5), where Z_{Fk} is the filter impedance between each inverter participating in the strategy (i.e. injecting a high frequency voltage/current) and the microgrid, Z_{Lk-1k} is the line impedance between nodes k–1 and k, Z_{lk} is the load impedance in node k, Z_g is the grid impedance and v_{hfk} is the high frequency voltage injected by the inverter at node k.

The model in Fig. 5 and (5) can be used to analyze the system response to the high frequency signals by just replacing the impedances and voltage sources by their corresponding high frequency values. As discussed for the models shown in Fig. 3, the grid voltage as well as the voltage for any generating unit or load not injecting the high frequency voltage/current can be made equal to zero, as they do not contain a high frequency component. Therefore, the grid as well as passive loads or generators are replaced by an equivalent impedance connected to ground. As consequence of this, the grid impedance Z_g is connected to ground in the grid side and is *measurable* (see Fig. 5). This is true even in the event that no net power flows through the PCC in grid operation (the microgrid voltage at the PCC in island condition exactly matches the grid voltage). It is also noted that the model presented in Fig. 5 assumes that there is a load connected at each node. This corresponds to the *microgrid* case discussed in Section I. The model in Fig. 5 and (5) can be easily adapted to the *multi-inverter* case discussed in section I by making the load impedances equal to infinity. This is the case when most or all of the power is evacuated to the grid at the PCC (e.g. distributed photovoltaic generation systems [24]).

It is finally noted that (5) assumes that the inverters operate as a *voltage source*. For inverters operating in the *current source* mode, (5) can be algebraically rearranged by moving the corresponding current i_{Fk} to the left term (inputs vector) and the inverter voltage v_{hfk} to the right side (outputs vector) of the equation respectively.

b) Combined high frequency voltage/current signal injection

A means to combine current and voltage injection is to use a *realizable references* anti-windup strategy [25]. This is schematically shown in Fig. 6. The high frequency current magnitude i_{hfmax} is commanded to a synchronous PI current regulator rotating at ω_{hf} (see (1) and Fig. 6). If the voltage required to supply the commanded current is lower than the established voltage limit, i.e. $v_{hf}^{*}<v_{hfmax}$, the current injection mode works normally. This will occur when Z_{hf} is small. On the contrary, if the $v_{hf}^{*}>v_{hfmax}$, the voltage is limited to v_{hfmax}. This will occur when Z_{hf} is large. The *realizable references* block in Fig. 6 guarantees a smooth transition between both modes of operation [25].

Fig. 7 schematically shows the injected high frequency voltage at the inverter terminals (commanded), the high frequency voltage at the filter output and the resulting high frequency current, as a function of the filter impedance vs. equivalent high frequency impedance ratio. When the impedance Z_{hf} is large the inverter output voltage is limited, i.e. it operates as a *voltage source*. As Z_{hf} decreases (Z_F/Z_{hf} increases), once the high frequency current reaches its rated value the inverter works as a *current source*.

For the implementation of the strategy, i_{hfmax} is selected first. The relationship between i_{hfmax} and v_{hfmax} is set to be (6), where Z_F is the (known) filter impedance and $\hat{Z}_{hf}$ is the preset value of the high frequency impedance at which the change between *voltage source* and *current source* occurs. For the simulation and experiments carried out in this paper, i_{hfmax} was set to 1.5% of the rated current and $\hat{Z}_{hf} = 0.35 \cdot Z_F$, v_{hfmax} being obtained from (6).

$$v_{hfmax} = i_{hfmax} (Z_F + \hat{Z}_{hf}) \tag{6}$$

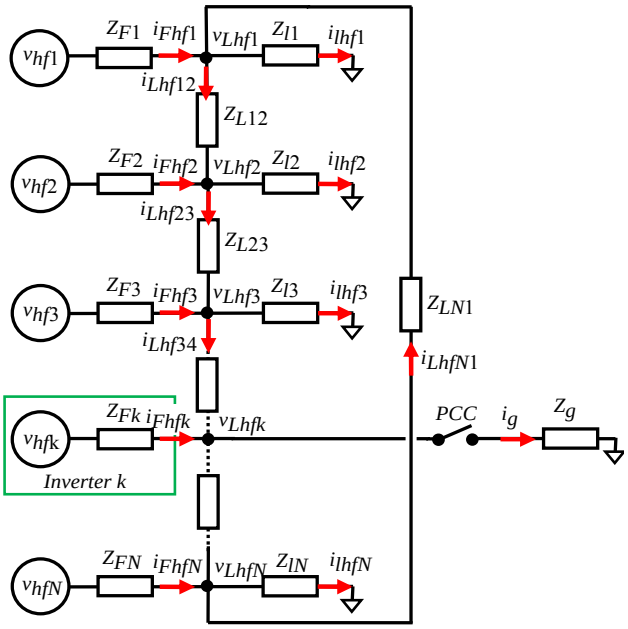

Fig. 5.- Generic microgrid architecture.

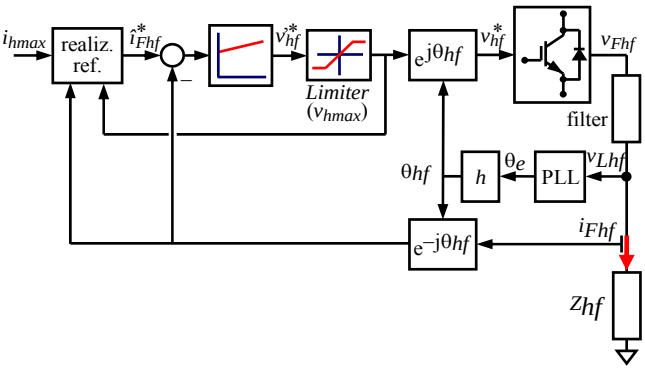

Fig. 6.- Power converter, including high frequency current regulator, *realizable references* block, and PLL for the synchronization of the high frequency signal with the grid fundamental voltage.

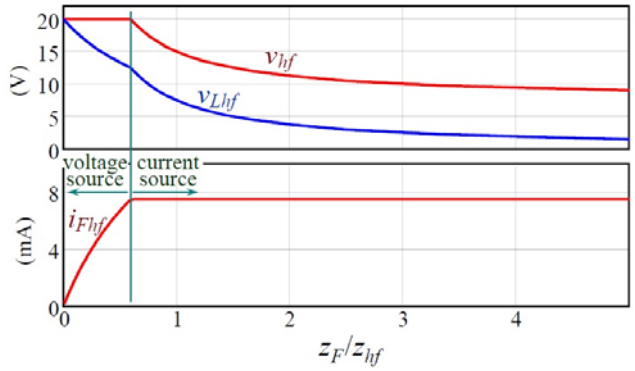

Fig. 7.- Combined *voltage source* and *current source* modes of operation.

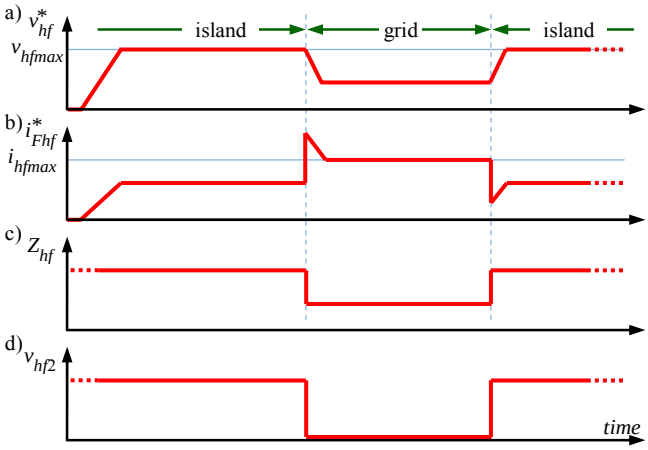

Fig. 8.- Schematic representation of the transition between island and grid conditions. a) Magnitude of the high frequency voltage and b) current injected for islanding detection; c) high frequency impedance; d) secondary high frequency voltage.

Fig. 8 shows the simulated response of the method. For island mode, the voltage is limited (Fig. 8a). For grid operation, the impedance seen by the inverter is small and current injection works normally. The high frequency current command is equal to the nominal value i_{hfmax}. It is remarked that the transition between *voltage* and *current source* modes occurs smoothly, no reconfiguration of the high frequency signal injection mechanism being needed (Fig. 8c). Experimental results showing the operation of this method are provided in Section V.

c) Synchronization of the high frequency signal injection

If multiple inverters inject simultaneously, synchronization of the high frequency signal for each inverter is highly advisable. This will reduce the *differential* high frequency voltage among inverters. Otherwise, the resulting differential high frequency voltage will cause high frequency currents circulating among the inverters. This will adversely affect to the power quality (THD), also making more challenging the detection of grid/island condition.

Phase-synchronization of the inverters can be done by selecting the high frequency voltage to be an integer multiple of the grid frequency. A cascade complex coefficient filter with complex *PLL* (CCCF-CPLL) [26] was used for this purpose (see Fig. 6).

Errors in the synchronization of the high frequency signals are likely to occur in practice due to several reasons. Differences in the voltage angle in different parts of the network and/or harmonics/unbalances in the grid voltage can affect to the PLL angle estimation and produce an unsynchronized injection of the high frequency voltages. Adverse effects of this would include errors in the estimated high frequency impedance and an increase of the THD due to high frequency currents circulating among the inverters.

Errors due to differences in the voltage angle are expected to be of little importance in practice. **T**he angle difference will be small for inverters operating near to each other. For inverters located farther away from each other, the angle difference and the impedance between the inverters will increase nearly proportionally, roughly cancelling to each other. It is also noted in this regard that in networks spread over a smaller area, the impedances are still inductive but have a significant resistive component [1].

A similar argumentation can be used to analyze the effects of harmonics/unbalances. Neighboring inverters should experience similar disturbances and react in a similar manner, thus limiting the risk of differential high frequency voltages among inverters. However, the behavior in this case will strongly depend on the PLLs response (bandwidth, harmonic rejection capability, etc). Inverters with different PLL designs might respond differently to harmonics, transients, etc., increasing the risk of interference. A thorough analysis of this issue has not been carried out yet.

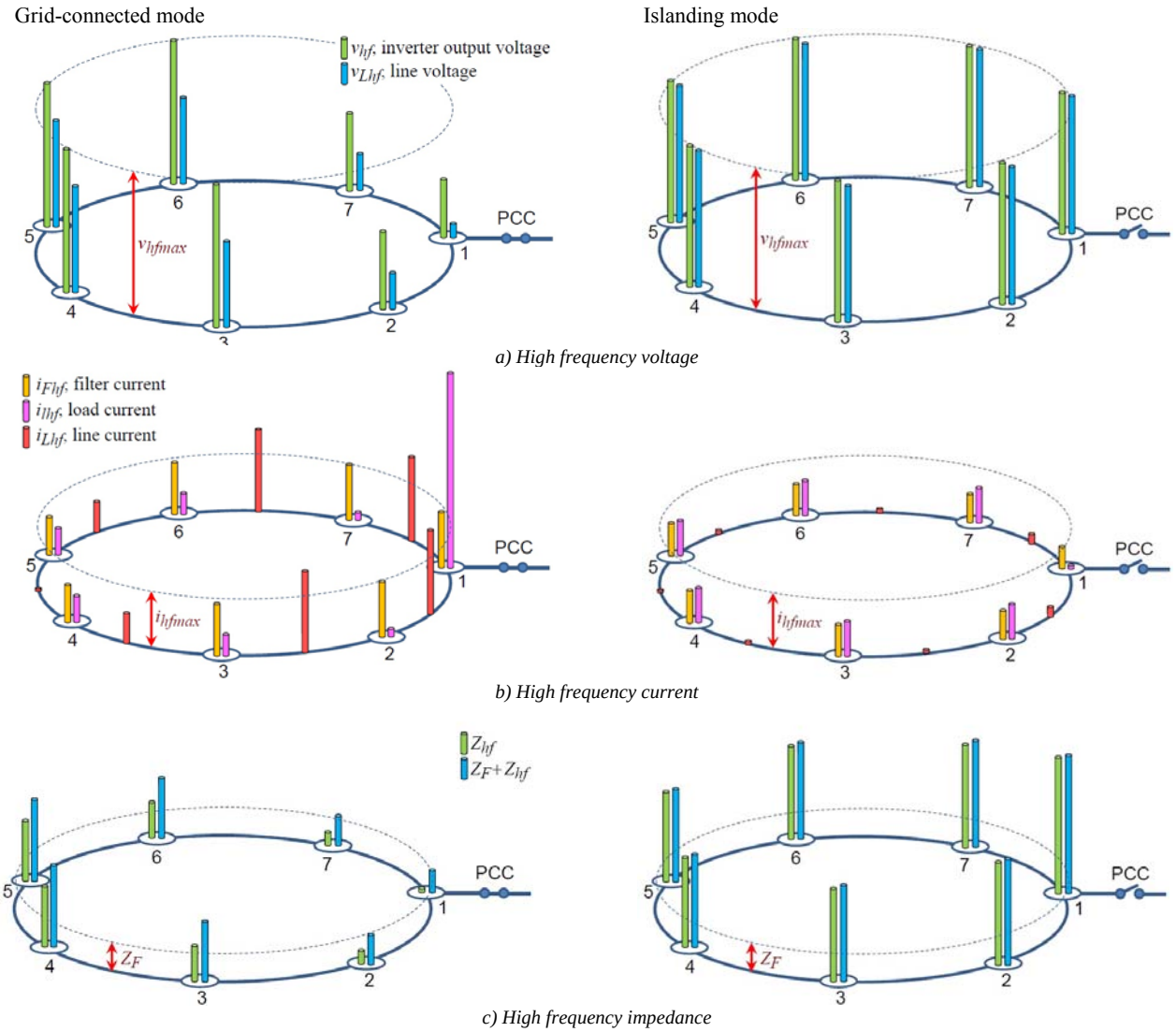

Fig. 9.- Schematic representation of the microgrid, operating in grid-connected (left) and islanding (right) modes. a) high frequency voltages, b) high frequency currents and c) high frequency impedances. The load current in node #1 corresponds to the high frequency current circulating into the grid. The bars in subplots a) to b) are referred to the maximum high frequency voltage v_{hfmax}, current i_{hfmax} and output filter impedance Z_F, respectively.

d) Parallel operation of the inverters

Inverters using the combined *voltage source*/*current source* modes can be directly connected in parallel. The result is a microgrid in which all the inverters participating in the islanding detection strategy inject the high frequency signal. Each inverter automatically selects the mode of operation as a function of the high frequency impedance Z_{hf} present at its terminals. Fig. 9 show an example obtained using the model in Fig. 5, (5) for the case of grid (left) and island operation (right). In the example shown in Fig. 9, the microgrid consists of seven nodes radially connected with the PCC connected to node #1. Each inverter uses the configuration shown in Fig. 6. The system parameters are the same as for the experimental results (see Table I). The bars in Fig. 9a show the inverter output voltage v_{hf} and line voltage v_{Lhf} (filter output voltage) for each node. Fig. 9b shows the filter, line and load high frequency current. The limits for the high frequency voltage v_{hfmax} and current i_{hfmax} are indicated in Fig. 9a and 8b (see Fig. 7 and 7). Node #1 corresponds to the PCC, the load current in this node coinciding therefore with the high frequency current circulating into the grid.

It is observed from Fig. 9a-left and 9b-left that for grid-connected case inverters in nodes #1, #2, and #7 operate in the *current source* mode. Due to their closeness to the PCC the impedance seen by these inverters is small, their high frequency current being limited to i_{hfmax}. On the contrary,

nodes #3 to #6 operate in the *voltage source* mode as they are further from the PCC. It is remarked again that the transition between *voltage source* and *current source* occurs smoothly, no reconfiguration of the injection mechanism being needed.

Table I. Experimental setup parameters	
Grid	380 V, 50 Hz, S_{cc}=2 MVA
Inverters	380 V, 30 kVA, 10 kHz.
Load	15 kW
v_{hfmax}	13 V (0.0325 pu), 250 Hz (5✕ω_e)
i_{hfmax}	1 A (0.0155 pu)
Line impedance Z_L	2Ω
LCL filter	2.4/2.3 mH (inverter/grid side), C=30uF

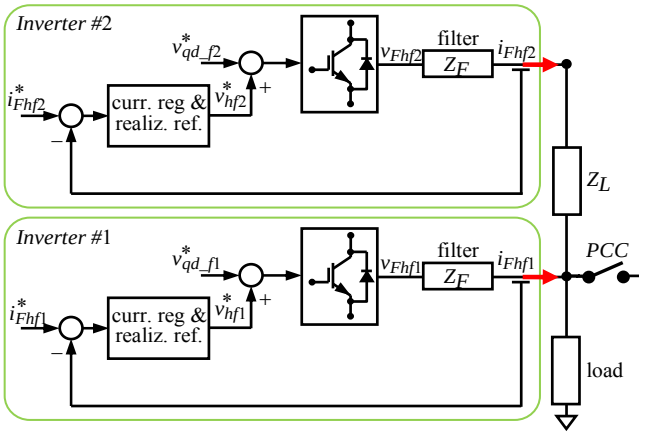

Fig. 10.- Experimental setup, consisting of two inverters. Current regulators needed for the control of the fundamental current are not shown.

e) Islanding detection and islanding notification

Islanding is detected from the measured high frequency impedance. Fig. 9c shows the high frequency impedance seen at the inverters terminal (7) and filters output (8).

$$Z_F + Z_{hf} = \frac{v_{hf}}{i_{Fhf}} \approx \frac{v^*_{hf}}{i_{Fhf}} \tag{7}$$

$$Z_{hf} = \frac{v_{Lhf}}{i_{Fhf}} \tag{8}$$

Since Z_{hf} is the variable reflecting the changes between grid and islanding modes, (8) would be used in principle for islanding detection. However, using (7) has the advantage that the commanded high frequency voltage can be used instead of the high frequency component of the measured line voltage needed in (8). This slightly simplifies the required signal processing. Still both options are expected to give similar results.

Some expected facts are observed in Fig. 9. For the case of grid-connected operation, the high frequency impedances for each node (both Z_{hf} and $Z_F + Z_{hf}$ in Fig. 9c) depend on the node location relative to the PCC. The impedances for nodes closer to the PCC are significantly smaller. The largest variations of the high frequency impedance between grid (Fig. 9c-left) and island connection (Fig. 9c-right) occur at nodes closer to the PCC.

Islanding detection is currently based on the rate of variation of Z_{hf} with time, i.e. $\Delta Z_{hf}/\Delta t$ [4-13]. Comparison of Z_{hf} with a threshold might also potentially be used [21]. Islanding detection will be easier and more reliable for nodes closer to the PCC. On the contrary, islanding detection might be difficult for nodes far from the PCC in large microgrids. Thus, inverters working in the *current source* mode would be in principle better candidates to detect islanding than inverters working in the *voltage source* mode.

A possible strategy would be to enable only inverters working in the *current source* to *inform* on the grid condition to the rest of inverters present in the microgrid. A secondary high frequency signal would be for this purpose. Inverters working in the *current source* mode would detect islanding by measuring a positive ΔZ_{hf} over a predefined time window. Once islanding is detected, they would inject the secondary high frequency signal v_{hf2}. On the contrary, if inverters injecting the secondary high frequency voltage detect the change between islanding and grid-mode from the measured ΔZ_{hf}, they would discontinue injecting the secondary high frequency voltage. Injection of the secondary high frequency voltage is schematically shown in Fig. 8d. Details on the use of the method can be found in [21,22]. This strategy has not been studied in detail, further analysis would be needed to verify its viability and performance.

V.- Experimental results

The proposed islanding detection strategy has been tested using the experimental setup shown in Fig. 10. The parameters are summarized in Table I. Both inverters are identical and use IGBTs. All the control (current regulators, synchronization, etc.) is implemented on a TMS320F28335 DSP.

Fig. 11 shows the transition between island and grid modes. Fig. 11a and 11c show the commanded and filter output voltages for both inverters. Fig. 11b and 11d show the corresponding high frequency currents. The magnitude of the high frequency current i_{hfmax} is set to 1 A (1.5% rated current). It is observed from Fig. 11b that during islanding both inverters operate in the *voltage source* mode, with v_{hfmax} = 13 V. During island operation Inverter #1 changes its mode of operation to the *current source* mode, the high frequency current magnitude being limited to i_{hfmax}. Inverter #2 keeps operating in the *voltage source* mode. This is due to the line impedance between Inverter #2 and the PCC.

Fig. 11e show the magnitude of the corresponding high frequency impedances. It is observed that for this particular case the change between grid and island modes is readily detected by both inverters. This is due to the fact that the line impedance Z_L is small compared to the impact that the change between grid and island operation has on the equivalent impedance Z_{hf}. It is noted however that, for the case of large microgrids, inverters far from the PCC might experience

significantly smaller variations of the equivalent impedance. This will make them less reliable for islanding detection.

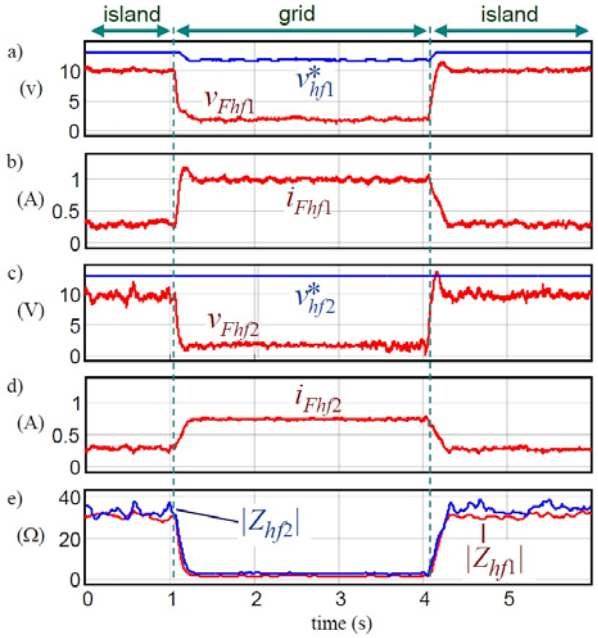

Fig. 11.- Experimental results showing the response of the proposed method during island-grid transitions.

VI.- Conclusions

A method to detect islanding in grids with multiple parallel-connected inverters has been presented in this paper. In the proposed method, all the inverters participating in the strategy inject the high frequency signal. The inverters can operate in two different modes of operation: *Current injection* mode and *Voltage injection*. Combined used of these modes has two advantages: the adverse impact that the injection of the high frequency signal has on the power quality (THD) is limited and provides a mean to evaluate the suitability of a particular inverter to detect islanding, which can be important in large microgrids. An important feature of the proposed method is that transition between *current injection* and *voltage injection* modes of operation occurs automatically and smoothly, no change in the configuration of the inverters being required. Simulation and experimental results have been presented to demonstrate the viability of the proposed method.

References

[1] Guerrero, J.M.; Chandorkar, M.; 3, T.; Loh, P.C., " Advanced Control Architectures for Intelligent Microgrids—Part I: Decentralized and Hierarchical Control," *IEEE Trans. on Ind. Electr.*, vol.60, no.4, pp.1254,1262, April 2013

[2] Massoud, A.M.; Ahmed, K.H.; Finney, S.J.; Williams, B.W., "Harmonic distortion-based island detection technique for inverter-based distributed generation," IET Renewable Power Generation, vol.3, no.4, pp.493,507, December 2009

[3] J.M. Lee, Islanding Detection Methods for Microgrids, Ms. Thesis, University of Wisconsin-Madison, 2011

[4] IEEE, "IEEE Standard for Interconnecting distributed resources with electric power systems," IEEE Std. 1547, 2003.

[5] IEC, "IEC Photovoltaic (PV) systems. Characteristics of the utility interface," IEC Std. 61 727, 2004.

[6] ENEL, "DK 5940 Criteria for connection of generation systems to ENEL low voltage distribution networks," 2006.

[7] IEEE Std. 929-2000, *IEEE Recommended Practice for Utility Interface of Photovoltaic (PV) Systems*, IEEE Standards Coordinating Committee 21 on Photovoltaics, New York, NY, Apr. 2000.

[8] UL1741, *UL Standard for Safety for Static Converters and Charge Controllers for Use in Photovoltaic Power Systems*, Underwriters Laboratories, May 7, 1999, revised June 2001.

[9] IEC 62116, *Testing Procedure of Islanding Prevention Measures for Grid Connected Photovoltaic Power Generation Systems*, International Electrotechnical Commission.

[10] DIN-VDE, "Automatic Disconnection Device Between a Generator and the Low-Voltage Grid," DIN-VDE Std. 0126-1-1, 2005.

[11] G77 – Recommendations for the Connection of Inverter- Connected Single-Phase Photovoltaic (PV) Generators up to 5kVA to Public Distribution Networks.

[12] ÖVE/Önorm E 2750 "Photovoltaische Energieerzeugungsanlagen – Sicherheitsanforderungen ("Photovoltaic power generating systems – safety requirements").

[13] VSE Sonderdruck Abschnitt 12 'Werkvorschriften über die Erstellung von elektr. Installation' Elektrische Energieerzeugungsanlagen Completes VSE 2.8d-95.

[14] A. Timbus, A. Oudalov, C. N.M. Ho, "Islanding Detection in Smart Grids" IEEE-ECCE'10, pp.3631 – 3637, Sep. 2010.

[15] R. Teodorescu, M. Liserre, P. Rodriguez and F. Blaabjerg, Grid Converters for Photovoltaic and Wind Power Systems, Wiley-IEEE 2011.

[16] M. Ciobotaru, R. Teodorescu, P. Rodriguez, A. Timbus and F. Blaabjerg, "On-line Grid Impedance Estimation for Single Phase Grid-Connected Systems Using PQ Variations", IEEE-PESC, pp.2306–2312, June 2007.

[17] A. V. Timbus, R. Teodorescu and U. Borup, "Online Grid Impedance Measurement Suitable for Multiple PV Inverters Running in Parallel", IEEE-APEC'06, pp.907–911, March 2006.

[18] L. Asiminoaei, R. Teodorescu, F. Blaabjerg and U. Borup, "A Digital Controlled PV-Inverter with Grid Impedance Estimation for ENS Detection", IEEE Trans. on Ind. Appl., 20(4):1480–1490, Nov.-Dec. 2005.

[19] L. Asiminoaei, R. Teodorescu, F. Blaabjerg and U. Borup, "A New Method of On-Line Grid Impedance Estimation for PV Inverter", IEEE-APEC'04, pp.1527–1533, Sept. 2004.

[20] M. Ciobotaru, R. Teodorescu and F. Blaabjerg, "On-line Grid Impedance Estimation Based on Harmonic Injection for Grid-Connected PV Inverter", IEEE-ISIE, pp.2473–2442, June 2007.

[21] Reigosa, D.D.; Briz, F.; Charro, C.B.; Garcia, P.; Guerrero, J.M., "Active Islanding Detection Using High-Frequency Signal Injection, IEEE Trans. on Ind. Appl , vol.48, no.5, pp.1588,1597, Sept.-Oct. 2012

[22] Reigosa, D.; Briz, F.; Guerrero, J.; Garcia, P.; Blanco Charro, C., "Active Islanding Detection for Multiple Parallel-Connected Inverter-Based Distributed Generators Using High Frequency Signal Injection, IEEE Trans. on Power Electr., vol.29, no.3, pp.1192,1199, March 2014.

[23] Hernandez-Gonzalez, G.; Iravani, R., "Current injection for active islanding detection of electronically-interfaced distributed resources," IEEE Trans. on Power Delivery, vol.21, no.3, pp.1698-1705, July 2006

[24] Yan Zhou; Hui Li; Liming Liu, "Integrated Autonomous Voltage Regulation and Islanding Detection for High Penetration PV Applications", IEEE Trans. on Power Electr., vol.28, no.6, pp.2826,2841, June 2013

[25] Briz, F.; Diez, A.; Degner, M.W.; Lorenz, R.D., "Current and flux regulation in field-weakening operation, *IEEE Trans. on Ind. Appl.*, vol.37, no.1, pp.42,50, Jan/Feb 2001

[26] C. Blanco, D. Reigosa, F. Briz, J. M. Guerrero, y P. Garcia, "Grid synchronization of three-phase converters using cascaded complex vector filter PLL", in 2012 IEEE Energy Conversion Congress and Exposition (ECCE), pp. 196 –203, Sept. 2012.